Renormalization-group approach to the problem of conduction through a nanostructure

V. L. Campo, Jr. and L. N. Oliveira
Instituto de Física de São Carlos, Universidade de São Paulo, Caixa Postal 369, São Carlos, 13560-970 SP, Brazil
(Received 23 December 2002; published 31 July 2003)

We present a numerical renormalization-group computation of the zero-temperature conductance of a nanostructure coupled to two metallic leads. In our model, the leads are represented by conduction bands of noninteracting electrons and a single level containing up to two interacting electrons represents the nanostructure. The nanostructure energy is controlled by a gate potential V_g. We show that the frequency dependence of the linear conductance through the nanostructure can be computed from the impurity spectral density of the spin-degenerate Anderson model. We compute the latter numerically and determine (i) the frequency-dependent conductance for an illustrative value of V_g, and (ii) the zero-frequency conductance as a function of V_g.

DOI: 10.1103/PhysRevB.68.035337 PACS number(s): 75.30.Fv, 71.15.Mb, 75.50.Ee, 74.25.Ha

I. INTRODUCTION

Recent progress in semiconductor lithographic techniques has attracted much attention to the problem of electronic conduction through a nanostructure.[1–3] In spite of the extensive recent theoretical literature on the subject,[4–12] few quantitatively reliable results have been obtained. Qualitatively, it has long been understood that, due to the small capacitance of the nanostructure, the energy increment associated with the transfer of a single electron to or from the quantum dot is very large, and that this energy barrier tends to block conduction through the dot. Since the nanostructure potential can be controlled by the application of a gate voltage, this notion can be explored experimentally in a variety of arrangements. More recently, it was realized that at low temperatures, the Kondo effect[13] can hybridize different ground-state nanostructure occupancies and bypass this Coulomb blockade,[4] a finding that has been much discussed.[3] Approximate calculations studying the temperature and frequency dependence as well as the nonlinearity of the current-voltage characteristics of simple realistic models have appeared in print.

Here we present the first NRG computation of the frequency-dependent linear conductance through a nanostructure at zero temperature. Our results display the above-described features. In particular, for gate voltages such that, if the quantum dot were decoupled from the leads, its ground state would accomodate an odd number of electrons, we find that the Kondo effect allows conduction at low frequencies. For voltages such that the ground state would contain an even number of electrons, by contrast, the conductance drops to zero unless the frequency is sufficient to overcome the Coulomb blockade.[4]

In our model, the left and the right leads are represented by spin-degenerate conduction bands half-filled with noninteracting electrons and described by the dispersion relation ϵ_k. The quantum dot is mimicked by a single spin-degenerate level associated with the Fermi operator c_0. The model Hamiltonian is

$$H=\sum_{i,k}\ \epsilon_k c_{ki}^{\dagger}c_{ki}+\sum_{i,k}\ V_k(c_0^{\dagger}c_{ki}+\text{H.c.})+H_{dot}, \qquad (1)$$

where the Fermi operators c_{k_i} $(i=L,R)$ annihilate conduction electrons in the left $(i=L)$ and right $(i=R)$ leads. For briefness, we have left out the spin sums. The second term on the right-hand side couples the conduction states to the quantum dot; we assume that the couplings to the two leads are identical. The electronic interaction inside the dot is contained in the last term on the right-hand side:

$$H_{dot}=\epsilon_0 c_0^{\dagger}c_0+Un_{0\uparrow}n_{0\downarrow}, \qquad (2)$$

with $n_{0\mu}=c_{0\mu}^{\dagger}c_{0\mu}$.

Since the Hamiltonian is invariant under inversion, we find it convenient to define parity conserving operators, i. e., even and odd operators

$$c_{kg}=(c_{kR}+c_{kL})/\sqrt{2} \qquad (3)$$

and

$$c_{ku}=(c_{kR}-c_{kL})/\sqrt{2}, \qquad (4)$$

respectively.

Equation (1) then becomes

$$H=\sum_{p,k}\ \epsilon_k c_{kp}^{\dagger}c_{kp}+\sqrt{2}\sum_{k}\ V_k(c_0^{\dagger}c_{kg}+\text{H.c.})+H_{dot}, \qquad (5)$$

where the subscript $p=g,u$ denotes parity. We see that the quantum-dot state c_0 is decoupled from the odd states c_{ku}; this allows us to write

$$H=H_g+H_u, \qquad (6)$$

where

$$H_g=\sum_{k}\ \epsilon_k c_{kg}^{\dagger}c_{kg}+\sqrt{2}\sum_{k}\ V_k(c_0^{\dagger}c_{kg}+\text{H.c.})+H_{dot}, \qquad (7)$$

while

$$H_u=\sum_{k}\ \epsilon_k c_{ku}^{\dagger}c_{ku} \qquad (8)$$

is diagonal.

This decoupling between the odd conduction states and the quantum dot level has a number of important consequences. In particular, the number of odd conduction electrons is conserved, a feature that will substantially simplify our analysis.

Under experimental conditions, it is virtually impossible to construct leads that couple identically to the nanostructure. One might want, therefore, to consider unequal couplings, i. e., a model that is asymmetric under inversion. Even in that case, however, it is possible to decompose the conduction bands into two channels, one of which is decoupled from the dot. Inversion symmetry is therefore unessential to our approach. It does, however, make our treatment simpler and physically more appealing; for this reason, we prefer to consider the symmetric model. For future reference, then, we find it convenient to split the even-channel Hamiltonian in three terms:

$$H_g = H^g_{CB} + H_c + H_{dot}, \tag{9}$$

where

$$H^g_{CB} = \sum_k \epsilon_k c^\dagger_{kg} c_{kg}, \tag{10}$$

is the even conduction-band Hamiltonian,

$$H_c = \sqrt{2} \sum_k V_k (c^\dagger_0 c_{kg} + \text{H.c.}), \tag{11}$$

couples the quantum-dot to the (even channel of the) conduction band, and H_{dot} is given by Eq. (2).

Our computation of the linear ac conductance starts out with an expression distilled from the Kubo formula[14]

$$\Re G(\omega) = \frac{e^2\pi}{Z4\omega} \sum_{m,n} (e^{-\beta E_n} - e^{\beta E_m}) \times |\langle m|\dot{N}_R - \dot{N}_L|n\rangle|^2 \delta(\hbar\omega - E_{mn}), \tag{12}$$

where the $E_{mn} = E_m - E_n$ are differences between eigenvalues of H, and N_L and N_R are the electronic number operators for the left and the right lead, respectively. The time derivatives $\dot{N}_L$ and $\dot{N}_R$ are easily computed. We have that

$$\dot{N}_R - \dot{N}_L = \frac{1}{i\hbar}[H, N_R - N_L], \tag{13}$$

from which it follows that

$$\dot{N}_R - \dot{N}_L = \frac{1}{i\hbar} \sum_k V_k (c^\dagger_0 c_{kR} - c^\dagger_0 c_{kL}) + \text{H.c.}, \tag{14}$$

or, as follows from Eq. (4),

$$\dot{N}_R - \dot{N}_L = \sqrt{\frac{2}{i\hbar}} \sum_k V_k c^\dagger_0 c_{ku} - \text{H.c.} \tag{15}$$

The conductance [Eq. (12)], becomes

$$\Re G(\omega) = \frac{e^2\pi}{Z2\hbar^2\omega} \sum_{m,n} (e^{-\beta E_n} - e^{-\beta E_m}) \times \left| \sum_k V_k \langle m|c^\dagger_0 c_{ku} - c^\dagger_{ku} c_0|n\rangle \right|^2 \delta(\hbar\omega - E_{mn}). \tag{16}$$

The conservation of particles in the odd channel guarantees that, for given eigenstates $|m\rangle$ and $|n\rangle$, at least one of the matrix elements $\langle m|c^\dagger_0 c_{ku}|n\rangle$ and $\langle m|c^\dagger_{ku} c_0|n\rangle$ will vanish. The right-hand side of Eq. (16) can therefore be divided into two sums:

$$\Re G(\omega) = \frac{e^2\pi}{Z2\hbar^2\omega} \left\{ \sum_{m,n} (e^{-\beta E_n} - e^{-\beta E_m}) \times \sum_k |V_k|^2 |\langle m|c^\dagger_0 c_{ku}|n\rangle|^2 \delta(\hbar\omega - E_{mn}) + \sum_{m,n} (e^{-\beta E_n} - e^{-\beta E_m}) \times \sum_k |V_k|^2 |\langle m|c^\dagger_{ku} c_0|n\rangle|^2 \delta(\hbar\omega - E_{mn}) \right\}. \tag{17}$$

Next, we exchange the dummy variables m and n in the first sum on the right-hand side. This leads to

$$\Re G(\omega) = \frac{e^2\pi}{Z2\hbar^2\omega} \left\{ \sum_{m,n} (e^{-\beta E_n} - e^{-\beta E_m}) \times \sum_k |V_k|^2 |\langle m|c^\dagger_0 c_{ku}|n\rangle|^2 \delta(\hbar\omega - E_{mn}) \right. \tag{18}$$

$$\left. + \sum_{m,n} (e^{-\beta E_m} - e^{-\beta E_n}) \times \sum_k \left| V_k \right|^2 \left| \langle m|c^\dagger_0 c_{ku}|n\rangle \right|^2 \delta(\hbar\omega - E_{nm}) \right\}, \tag{19}$$

and hence to

$$\Re G(\omega) = \frac{e^2\pi}{Z2\hbar^2\omega} \sum_{mnk} (e^{-\beta E_n} - e^{-\beta E_m}) |V_k|^2 \times |\langle m|c^\dagger_{ku} c_0|n\rangle|^2 [\delta(\hbar\omega - E_{mn}) - \delta(\hbar\omega - E_{nm})]. \tag{20}$$

As follows from the decoupling between the even and the odd channel in Eq. (6), the eigenstates $|m\rangle$ of the model Hamiltonian can be written as $|m_g\rangle|m_u\rangle$, where $|m_g\rangle$ and $|m_u\rangle$ are eigenstates of the even and the odd Hamiltonians, H_g and H_u, respectively. We thus have that

$$H|m\rangle = (E_{m_g} + E_{m_u})|m\rangle, \tag{21}$$

where E_{m_g} and E_{m_u} are the energies of the states $|m_g\rangle$ and $|m_u\rangle$, respectively. The matrix elements on the right-hand side of Eq. (16) can be simplified:

$$\langle m|c_{ku}^{\dagger}c_0|n\rangle\langle m_u|c_{ku}^{\dagger}|n_u\rangle\langle m_g|c_0|n_g\rangle. \tag{22}$$

Since the c_{k_u} diagonalize the odd-channel Hamiltonian H_u, the first matrix element on the right-hand side will vanish unless $|m_u\rangle = c_{ku}^{\dagger}|n_u\rangle$, and then

$$E_{m_u} = E_{n_u} + \epsilon_k \tag{23}$$

and

$$\langle m_u|c_{ku}^{\dagger}|n_u\rangle = 1. \tag{24}$$

With these simplifications, Eq. (20) becomes

$$\Re G(\omega) = \frac{e^2\pi}{Z2\hbar^2\omega}\sum_{m_g n_g k}\sum_{m_u}{}' e^{-\beta E_{m_u}}[e^{-\beta(E_{n_g}-\epsilon_k)} - e^{-\beta E_{m_g}}]|V_k|^2|\langle m_g|c_0|n_g\rangle|^2[\delta(\hbar\omega - E_{m_g n_g} - \epsilon_k) - \delta(\hbar\omega - E_{n_g m_g} + \epsilon_k)], \tag{25}$$

where the primed sum includes only those odd eigenstates $|m_u\rangle$ in which the k state is occupied.

It is now a simple matter to evaluate a partial trace, over the odd-channel states. This leads to

$$\Re G(\omega) = \frac{e^2\pi}{Z_g 2\hbar^2\omega}\sum_{m_g n_g k}[e^{-\beta(E_{n_g}-\epsilon_k)} - e^{-\beta E_{m_g}}] \times |V_k|^2|\langle m_g|c_0|n_g\rangle|^2 f(\epsilon_k) \times [\delta(\hbar\omega - E_{m_g n_g} - \epsilon_k) - \delta(\hbar\omega - E_{n_g m_g} + \epsilon_k)]. \tag{26}$$

Here Z_g is the even-channel partition function and $f(\epsilon)$ is the Fermi function.

Compare, next, the right-hand side to the definition of the dot-level spectral density,[15]

$$\rho(\epsilon) = \frac{1}{Z_g}\sum_{m_g n_g}(e^{-\beta E_{m_g}} + e^{-\beta E_{n_g}}) \times |\langle m_g|c_0|n_g\rangle|^2\delta(\epsilon - E_{n_g m_g}), \tag{27}$$

which we prefer to write

$$f(-\epsilon)\rho(\epsilon) = (1+e^{-\beta\epsilon})\frac{1}{Z_g}\sum_{m_g n_g} e^{-\beta E_{m_g}} \times |\langle m_g|c_0|n_g\rangle|^2\delta(\epsilon - E_{n_g m_g}). \tag{28}$$

Substitution in Eq. (26) then yields

$$\Re G(\omega) = \frac{e^2\pi}{2\hbar^2\omega}\sum_k |V_k|^2 f(\epsilon_k)[(e^{\beta\hbar\omega}-1)f(\hbar\omega - \epsilon_k) \times \rho(-\hbar\omega + \epsilon_k) - (e^{-\beta\hbar\omega}-1)f(-\hbar\omega - \epsilon_k) \times \rho(\hbar\omega + \epsilon_k)] \tag{29}$$

or

$$\Re G(\omega) = \frac{e^2\pi}{2\hbar}\frac{1-e^{-\beta\hbar\omega}}{\hbar\omega}\sum_k |V_k|^2[f(-\epsilon_k)f(-\hbar\omega + \epsilon_k) \times \rho(-\hbar\omega + \epsilon_k) + f(\epsilon_k)f(-\hbar\omega - \epsilon_k)\rho(\hbar\omega + \epsilon_k)]. \tag{30}$$

At zero frequency, the two terms within the square brackets on the right-hand side become identical and we recover the well-established expression for the dc conductance.[4,16]

At zero temperature, the Fermi functions make the first (second) term within brackets on the right-hand side of Eq. (30) vanish unless $\hbar\omega \geq \epsilon_k \geq 0$ $(0 \geq \epsilon_k \geq -\hbar\omega)$. Our expression for the conductance reduces to

$$\Re G(\omega) = \frac{e^2\pi}{2\hbar^2\omega}\left[\int_0^{\hbar\omega}|V_k|^2\rho(-\hbar\omega + \epsilon_k)g(\epsilon_k)d\epsilon_k + \int_{-\hbar\omega}^{0}|V_k|^2\rho(\hbar\omega + \epsilon_k)g(\epsilon_k)d\epsilon_k\right], \tag{31}$$

where $g(\epsilon)$ denotes the conduction-band density of states.[17]

In the Kondo limit, a universal expression for the spectral density has been available for over a decade[13,18–21]:

$$\Gamma\rho(\epsilon) = \frac{2}{\pi}\Re\left\{\sqrt{\frac{i\Gamma_K}{\epsilon + i\Gamma_K}}\right\}, \tag{32}$$

where $\Gamma = 2\pi g(0)|V_{k_F}|^2$ is the width of the dot level, due to its coupling to the even conduction states, and the Kondo resonance width Γ_K is proportional to the Kondo temperature T_K,[22] $\Gamma_K = k_B T_K/0.206\pi$.

This is expression is valid for energies ϵ much smaller than the conduction bandwidth. For energies $\hbar\omega$ in the same range, we can substitute Eq. (32) for the spectral densities on the right-hand side of Eq. (31), neglect the momentum dependence of the coupling, $V_k \to V_{k_F}$, and neglect the energy dependence of the density of conduction states, $g(\epsilon) \to g(\epsilon_F \equiv 0)$. The resulting integrals are simple and lead to the following analytical expression for the zero-temperature frequency-dependent conductance:

$$\Re G(\omega) = \frac{e^2}{\pi\hbar}\sqrt{\frac{2}{1+\sqrt{1+(\hbar\omega/\Gamma_K)^2}}}. \tag{33}$$

As an illustration, following a procedure discussed in a number of papers,[18,20,23] we have carried out a numerical renormalization-group computation of the dissipative conductance. To calculate the conductance, we have derived an expression that is more practical, for numerical purposes, than computing the spectral density and then carrying out the

integration on the right-hand side of Eq. (31). Since the real part of the conductance is an even function of the frequency, it is sufficient to obtain that expression for $\omega>0$. Under this restriction, at zero temperature, Eq. (26) reduces to

$$\Re G(\omega>0)=\frac{e^2\pi}{2\hbar^2\omega}\sum_{m_g k}|V_k|^2[|\langle m_g|c_0|\Omega_g\rangle|^2\theta(\epsilon_k)\times\delta(\hbar\omega-E_{m_g}-\epsilon_k)+|\langle m_g|c_0^\dagger|\Omega_g\rangle|^2\theta(-\epsilon_k)\times\delta(\hbar\omega-E_{m_g}+\epsilon_k)]. \tag{34}$$

Here $|\Omega_g\rangle$ is the even-channel ground state, from which the energies E_{m_g} are measured. The momentum sum on the right-hand side is readily carried out and we find that

$$\Re G(\omega)=\frac{e^2\pi}{2\hbar^2\omega}\sum_{m_g}{}'\,[|\langle m_g|c_0|\Omega_g\rangle|^2 g(\epsilon_{k+})|V_{k+}|^2+|\langle m_g|c_0^\dagger|\Omega_g\rangle|^2|g(\epsilon_{k-})|V_{k-}|^2], \tag{35}$$

where the conduction energies ϵ_{k+} and ϵ_{k_-} are given by $\epsilon_{k+}\equiv-\epsilon_{k-}\equiv\hbar\omega-E_{m_g}$, and k_+ and k_- are the corresponding momenta, respectively, and the prime restricts the sum to those eigenstates $|m_g\rangle$ with energies smaller than $\hbar\omega$.

In order to evaluate the summand, we need the eigenvalues and eigenvectors of the even-channel Hamiltonian H_g, which is equivalent to the (single-channel) Anderson impurity Hamiltonian and is hence easily diagonalized by the NRG procedure.[24,25] Briefly described, that procedure comprises the following steps:

II. DISCRETIZATION OF THE CONDUCTION BAND

Assuming the band is half-filled, let it extend from $\epsilon_k=-D$ to $\epsilon_k=D$. For parameters Λ and z, subject to the restrictions $\Lambda>1$ and $0<z\leqslant 1$, but otherwise arbitrary, two infinite sequences of intervals $\epsilon_{m_+}\geqslant\epsilon_k>\epsilon_{m_++1}$ and $-\epsilon_{m_-+1}>\epsilon_k\geqslant-\epsilon_{m_-}$ $(m_\pm=0,1,\ldots)$ are defined, where $\epsilon_0=D$ and $\epsilon_{m_\pm}=D\Lambda^{1-z-m}$ $(m=1,2,\ldots)$. For each interval, a normalized Fermi operator $a_\pm$ is defined as the linear combination of the conduction operators c_{kg} in that interval that is most localized around the quantum dot site, $a_\pm=N_{m_\pm}\Sigma_k'c_{kg}$, where the prime restrics the sum to the $m_\pm$th interval. The basis of the discrete operators $a_\pm$ is incomplete with respect to that of the c_k's, but the calculated conductances converge so rapidly to the continuum limit $\Lambda\to1$ that even computations carried out with $\Lambda=10$ yield an excellent approximations to the continuum. When the even channel of the conduction band Hamiltonian,

$$H_{CB}^g=\sum_k\epsilon_k c_{kg}^\dagger c_{kg}, \tag{36}$$

is projected onto that basis, we find that

$$H_{CB}^g=\sum_{m=0}^{\infty}E_m[a_{m_+}^\dagger a_{m_+}-a_{m_-}^\dagger a_{m-}], \tag{37}$$

where $E_0=D(1+\Lambda^{-z})/2$, and for $m>0$, the discrete energies are $E_m=D\Lambda^{-m+1-z}(1+\Lambda^{-1})/2$ $(m=1,2,\ldots)$.

III. LANCZOS TRANSFORMATION

Applied to the Hamiltonian H_{CB}^g in Eq. (37), a Lanczos transformation defines a new orthonormal basis constituted by Fermi operators f_n $(n=0,1,\ldots)$. To construct this exact transformation, one requires that the even conduction Hamiltonian take the tridiagonal form

$$H_{CB}^g=\sum_{n=0}^{\infty}t_n(f_n^\dagger f_{n+1}+\text{H.c.}), \tag{38}$$

with appropriate coefficients t_n, and the following definition for the operator f_0:

$$f_0\equiv(1/V)\sum_k V_k c_{kg}, \tag{39}$$

where the mean-squared coupling $V=\sqrt{\Sigma_k V_k^2}$ in the denominator on the right-hand side normalizes f_0. The codiagonal coefficients t_n^z must be found numerically; for large n, nonetheless, one finds an approximate expression[23]

$$t_n^z=D_{n+1}\Lambda^{1-z}+\mathcal{O}(D\Lambda^{-n}), \tag{40}$$

where

$$D_n\equiv D\frac{1+\Lambda^{-1}}{2}\Lambda^{-(n-1)/2}. \tag{41}$$

For increasing n, the codiagonal coefficients thus decrease rapidly, a feature that paves the road to the truncation defined Sec. IV. Before coming to that, however, we remark that definition (39) allows us to rewrite Eq. (11) as

$$H_c=\sqrt{2}V(c_0^\dagger f_0+\text{H.c.}). \tag{42}$$

IV. INFRARED TRUNCATION

To calculate the ac conductance, we must compute the right-hand side of Eq. (35) as a function of the frequency ω. To this end, we have to diagonalize H_g, given by Eqs. (38) and (40). For given ω, we can neglect those codiagonal elements t_n that are much smaller than ω. We therefore choose a small number $\alpha\ll1$ and find the smallest integer N satisfying the inequality

$$D_N<\alpha\omega, \tag{43}$$

with D_N defined as in Eq. (41). Since $t_N\approx D_N\ll\omega$, we can truncate the sum on the right-hand side of Eq. (38) at $n=N$:

$$H_{CB}^g\approx\sum_{n=0}^{N-1}[t_n(f_n^\dagger f_{n+1}+\text{H.c.})], \tag{44}$$

an approximation referred to as the *infrared truncation*. This considered, to prepare a renormalization-group transformation, we define the scaled, truncated Hamiltonian

$$H_N^g = \left\{ \sum_{n=0}^{N-1} [t_n^z (f_n^\dagger f_{n+1} + \text{H.c.})] + \sqrt{2} V (c_0^\dagger f_0 + \text{H.c.}) + H_{dot} \right\} \Big/ D_N . \quad (45)$$

Here we have substituted the right-hand side of Eq. (42) for the coupling H_c between the dot and the conduction band.

From Eq. (45), the even-channel model Hamiltonian is formally recovered as

$$H_g = \lim_{\Lambda \to 1} \lim_{N \to \infty} D_N H_N . \quad (46)$$

Moreover, Eq. (45) leads to a renormalization-group transformation, that is, a transformation that, given a sequence of energies with a minimum E_{min}, adds to it a smaller energy $E'_{min} < E_{min}$ and scales up the entire sequence by the factor E_{min}/E'_{min}, so that the minimum of the resulting sequence be E_{min}, equal to the minimum of the original sequence. Specifically, the renormalization-group transformation associated with Eq. (45) is defined by

$$\mathcal{T}'[H_{N-1}] \equiv H_N = \Lambda^{1/2} H_{N-1} + (t_{N-1}/D_N)(f_N^\dagger f_{N-1} + \text{H.c.}). \quad (47)$$

As Eq. (41) shows, for increasing N, the factor multiplying the parentheses on the right-hand side becomes independent of N, so that the smallest energy scale in H_N is not significantly affected by the transformation. Eq. (40) defines a renormalization-group transformation that scales up energies by Λ.[25] An energy-scale invariant Hamiltonian is not affected by $\mathcal{T} = \mathcal{T}'^2$ and is called a fixed point. [Notice that, one cannot expect $\mathcal{T}'$ to have fixed points, for $\mathcal{T}'$ scales up energies by $\sqrt{\Lambda}$, while any two successive energies in the discretized conduction-band Hamiltonian (36) are separated by a factor Λ.]

V. ITERATIVE DIAGONALIZATION

Hamiltonian (45) is diagonalized iteratively. For $N=0$, the first term on the right-hand side vanishes, and the sum of two remaining can be diagonalized analytically. If, on the other hand, the eigenvalues ϵ_n and eigenvectors $|n\rangle$ of H_{N-1}^g are known, the states $|n\rangle$, $f_{N+1\uparrow}^\dagger |n\rangle$, $f_{N+1\downarrow}^\dagger |n\rangle$, and $f_{N+1\uparrow}^\dagger f_{N+1\downarrow}^\dagger |n\rangle$ constitute a new basis onto which H_N can be projected. Charge and spin conservation reduce that projection to a block-diagonal matrix that can be diagonalized numerically.

Thus, starting with $N=0$, one can diagonalize H_1, H_2, ... Since the number of states generated in each iteration N is four times larger than that in the previous iteration, computer memory limitations force us to truncate the basis. For each iteration with $N>5$, only the eigenvectors associated with the eigenvalues below a parameter ϵ_{lim} are computed in the numerical diagonalization, and those provide the seed from which the basis is constructed in the subsequent iteration. To distinguish this approximation from the one defined in Sec. IV, we refer to it as the *ultraviolet* truncation.

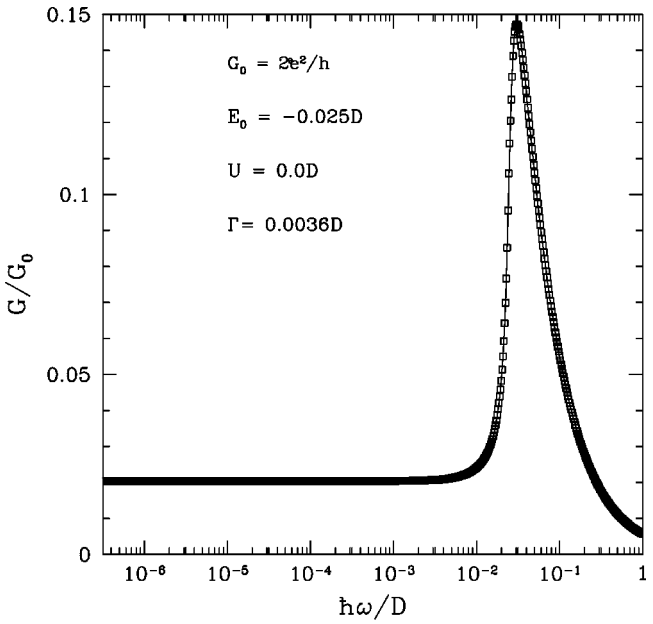

FIG. 1. Real part of the conductance as a function of frequency for the indicated dot energy E_0 and width Γ, for the uncorrelated model. The squares show the numerical results of the NRG procedure described in the text. The solid line represents the analytical expression for the conduction. The agreement is representative of the accuracy of all numerical results in this paper.

The discretization of the conduction band [Eq. (37)], which is controlled by the discretization parameter Λ, (ii) the infrared truncation [Eq. (38)], controlled by the parameter α, and the ultraviolet truncation, controlled by the parameter ϵ_{lim}, are the only approximations involved in the NRG procedure. The control over each approximation makes the procedure essentially exact.

VI. COMPUTATION OF THE z-DEPENDENT CONDUCTANCE

At iteration N, the numerical diagonalization of the model Hamiltonian yields eigenvalues that, in units of D_N [Eq. (41)], range from unity to ϵ_{lim}. For frequencies ω satisfying the inequality $1 < \hbar\omega/D_N < \epsilon_{lim}$, the sum on the right-hand side of Eq. (35) can be computed. By following the iterative procedure from $N=1$ to $N=N_{max}$, we calculate (the real part of the) conductance for frequencies in the interval $D_{N_{max}}/\hbar < \omega < D$. By choosing $N_{max}=21$, with $\Lambda=10$, for instance, we can reach frequencies as low as $\omega = 10^{-10} D/\hbar$, well below the characteristic energies of typical model Hamiltonians.

VII. AVERAGING OVER z

The discretization of the conduction band is an approximation. In order to justify it, one must insure that calculated physical properties converge rapidly to the continuum limit as $\Lambda \to 1$. The computation of dynamical properties, in particular, requires a special precaution: inspection of the right-hand side of Eq. (35) shows that for any $\Lambda > 1$ and fixed z,

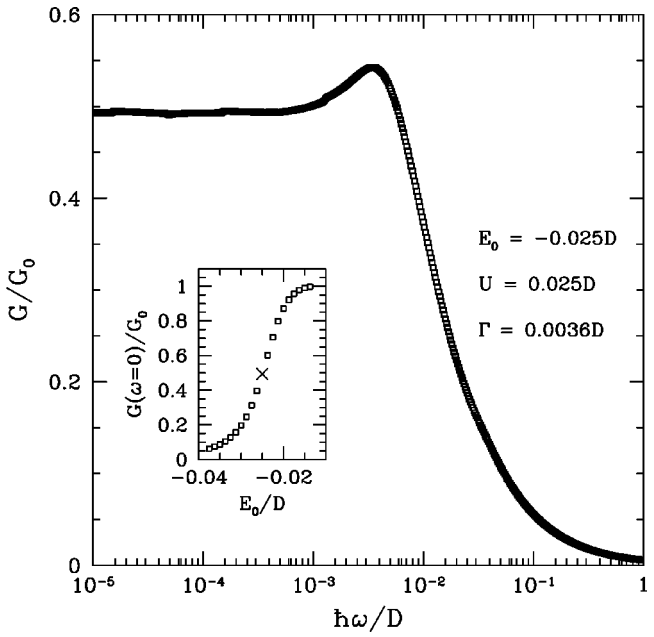

FIG. 2. Real part of the conductance as a function of frequency for the indicated dot energy E_0, width Γ and Coulomb repulsion U. Since $U=E_0$, for $\Gamma=0$ the dot states with occupancies $n=1$ and $n=2$ would be degenerate. The coupling to the conduction band breaks that degeneracy and allows transitions between the ground state and the resulting excited state, which enhance the spectral density and give rise to the peak in the conductance at $\hbar\omega\sim 6\times 10^{-3}D$. The inset shows the dc conductance as a function of the dot energy E_0; the cross indicates the $\omega\to 0$ limit of the main plot.

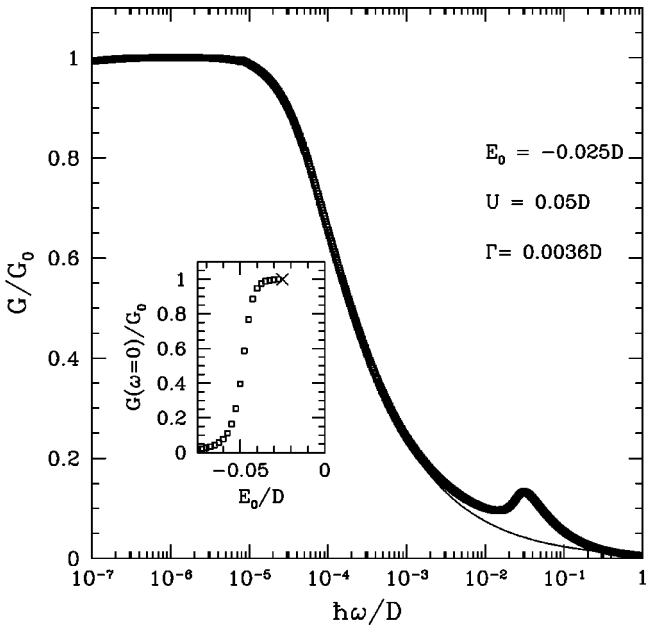

FIG. 3. Real part of the conductance as a function of frequency for the indicated dot energy E_0, width Γ and Coulomb repulsion U. With $U=2|E_0|$, the model becomes particle-hole symmetric and its low-energy physics is dominated by the Kondo effect. The two conductance peaks are associated with resonances in the dot-level spectral density. The peak at higher energies, near $\hbar\omega=|E_0|$, reflects the resonance associated with the transition between the $n_0=1$ and the $n_0=0$ and $n_0=2$ occupations of the dot level. The peak at zero frequency is due to the Kondo resonance, as confirmed by the excellent agreement with the exact result [Eq. (32)], here represented by the solid line. The inset shows the zero-frequency conductance as a function of E_0. The cross indicates the dc limit of the main plot.

the restricted sum over discrete energies will give rises to discontinuities in the calculated conductance $\Re G(\omega,z)$. In order to eliminate this artifact of the discretization, we must average $\Re G(\omega,z)$ over the second discretization parameter. As z runs from zero to unity, the energies E_m on the right-hand side of Eq. (36) sweep the entire conduction band and thus recover the continuous distribution of conduction energies.

For fixed z, the discontinuity in Eq. (35) arises because for given frequency ω one occasionally finds a state $|m_g\rangle$ with an energy E_{mg} slightly larger than $\hbar\omega$, which does not contribute to the sum on the right-hand side; in that case, for ω' slightly smaller than ω, the energy E_{mg} will be smaller than $\hbar\omega'$ and the state $|m_g\rangle$ will contribute to the sum, which is therefore discontinuous at $\hbar\omega=E_{mg}$. It is easy to see, however, that if for given z one has $E_{mg}(z)=\hbar\omega+\epsilon$, then for some $z'>z$ one will have that $E_{mg}(z')<\hbar\omega$, so that when the sum on the right-hand side of Eq. (35) is integrated over z the state $|m_g\rangle$ will contribute to the conductance, and the discontinuity will be washed out. We therefore expect the z-integrated conductance

$$\Re G(\omega)=\int_0^1 \Re G(\omega,z)dz, \tag{48}$$

to be a continuous function of the frequency that converges rapidly to the continuum limit as $\Lambda\to 1$. This is borne out by the numerical results.

VIII. RESULTS

Figure 1 shows the calculated conductance for $U=0$, with dot energy $\epsilon_0=-0.025\,D$ and width $\Gamma=0.0036\,D$. The conductance peaks near $|E_0|$, as the external frequency yields the electrons on the left lead sufficient energy to overcome the barrier separating the quantum dot from the two electron gases. The coupling to the electron gases broadens the resonance to a width approximately equal to Γ. The calculated conductances are in excellent agreement with the analytical expression easily derived in the absence of correlation,

$$\Re G(\omega)=\frac{\Gamma}{2\hbar\omega}\left[\arctan\left(\frac{\hbar\omega+\epsilon_0}{\Gamma}\right)+\arctan\left(\frac{\hbar\omega-\epsilon_0}{\Gamma}\right)\right], \tag{49}$$

represented by the continuous line.

While correlation makes it impossible to determine analytical expressions for the frequency-dependent conductance, the special precautions taken in the NRG approximations make that approach uniformly accurate in parametrical space; we hence expect the results for $U\neq 0$ to be as accurate as those in Fig. 1. As an illustration, Fig. 2 shows the calculated conductance for the dot energy and width in Fig. 1 and

$U=|E_0|=0.025D$. A comparison with Fig. 1 shows that the correlation displaces the peak to a lower energy and raises the dc conductance. Both effects are easy to understand if one considers that, for $U=0$, the decoupled-dot ground state would be doubly occupied, while for $U=|E_0|$, the doubly and singly occupied configurations would be degenerate. One might therefore expect free current flow at low energies, since that degeneracy would allow unassisted transitions between the dot and the neighboring gases. The coupling Γ breaks the degeneracy, so that only virtual transitions become possible at zero frequency, and the conductance peaks at the resonance associated with the broken degeneracy.

An additional check on the accuracy of our procedure is provided by the insert, which shows the dc conductance extracted from the ground-state occupancy of the quantum dot by means of the Friedel sum rule as a function of the dot energy E_0. The results, shown as open squares, are in very good agreement with the zero-frequency limit of the main plot, represented by the cross.

For $U=2|E_0|$, the model acquires particle-hole symmetry. This forces the dot occupation to be $n_0=1$. It follows from the Friedel sum rule that the dot density of states at the Fermi level is equal to $2\pi/\Gamma$,[18] and from Eq. (31) that $\Re G(\omega)=2e^2/\hbar$, which is just the dc limit of Eq. (32).

Figure 3 shows numerical results for the frequency dependence of the conductance for the symmetric model. The peak near $\hbar\omega=0.025D$ is due to the enhancement in the quantum-dot spectral density at energy $\epsilon\approx|E_0|$, associated with transitions from the singly occupied ground state to the (degenerate) doubly occupied and empty dot-level configurations. At lower frequencies, the calculated points are in excellent agreement with Eq. (32), represented by the continuous line. Again, the dc conductance extracted from the ground-state occupancy (open squares in the inset) agrees very well with the zero-frequency limit of the main plot (cross).

IX. CONCLUSIONS

In summary, we have shown that the NRG approach gives quantitatively reliable results for the frequency dependence of the (real part of) the conductance through a nanostructure. As indicated by Figs. 1 and 3, the agreement with exact results, where the latter are available, is excellent. This test highlights the adequacy of the NRG approach for the calculation of transport properties in devices dominated by the Coulomb blockade. Of particular interest is the computation of the current resulting from subjecting the electrodes to a noninfinitesimal potential difference. This arrangement poses a substantially more difficult problem than the one with which we have dealt. Nonetheless, inroads for renormalization-group analyses of nonequilibrium problems have been constructed,[26] and the above-reported analysis may encourage additional efforts.

ACKNOWLEDGMENT

This work was supported by the Brazilian agencies CAPES, CNPq and FAPESP.

[1] T. Inoshita, Science **281**, 526 (1998).
[2] D. Goldhaber-Gordon *et al.*, Phys. Rev. Lett. **81**, 5225 (1998).
[3] B.G. Levi, Phys. Today **51**(1), 17 (1998).
[4] T.K. Ng and P.A. Lee, Phys. Rev. Lett. **61**, 1768 (1988).
[5] M.H. Hettler, J. Kroha, and S. Hershfield, Phys. Rev. B **58**, 5649 (1998).
[6] W. Izumida, O. Sakai, and Y. Shimizu, J. Phys. Soc. Jpn. **67**, 2444 (1998).
[7] V.V. Kuznetsov *et al.*, Phys. Rev. B **56**, R15 533 (1997).
[8] A. Oguri, Phys. Rev. B **56**, 13 422 (1997).
[9] T. Ivanov, Europhys. Lett. **40**, 183 (1997).
[10] T. Pohjola *et al.*, Europhys. Lett. **40**, 189 (1997).
[11] C.W.J. Beenakker, Rev. Mod. Phys. **69**, 731 (1997).
[12] M.A. Davidovich, E.V. Anda, J.R. Iglesias, and G. Chiappe, Phys. Rev. B **55**, R7335 (1997).
[13] A.C. Hewson, *From the Kondo Problem to Heavy Fermions* (Cambridge University Press, Cambridge, 1993).
[14] W. Izumida, O. Sakai, and Y. Shimizu, J. Phys. Soc. Jpn. **66**, 717 (1997).
[15] G.D. Mahan, *Many-Particle Physics*, 2nd ed. (Plenum, New York, 1990).
[16] S. Hershfield, J.H. Davies, and J.W. Wilkins, Phys. Rev. Lett. **67**, 3720 (1991); Y. Meir and N.S. Wingreen, *ibid.* **68**, 2512 (1992); P.A. Lee, Physica B **189**, 1 (1993).
[17] In the case of electrodes with different couplings to the nanostructure, an additional term arises on the right-hand side of Eq. (30), which breaks the proportionality between the conductance and the dot spectral density. This term, however, is proportional to the difference between couplings and to the frequency, and hence typically very small.
[18] H.O. Frota and L.N. Oliveira, Phys. Rev. B **33**, 7871 (1986).
[19] R.N. Silver, J.E. Gubernatis, D.S. Sivia, and M. Jarrell, Phys. Rev. Lett. **65**, 496 (1990).
[20] L.N. Oliveira, V.L. Libero, H.O. Frota, and M. Yoshida, Physica B **171**, 61 (1991).
[21] M. Jarrell and J.E. Gubernatis, Phys. Rep.-Rev. Sec. Phys. Lett. **269**, 134 (1996).
[22] L.N. Oliveira and J.W. Wilkins, Phys. Rev. Lett. **47**, 1553 (1981).
[23] M. Yoshida, M.A. Whitaker, and L.N. Oliveira, Phys. Rev. B **41**, 9403 (1990).
[24] K.G. Wilson, Rev. Mod. Phys. **47**, 773 (1975).
[25] H.R. Krishna-murthy, J.W. Wilkins, and K.G. Wilson, Phys. Rev. B **21**, 1003 (1980).
[26] T.A. Costi, Phys. Rev. B **55**, 3003 (1997).